Journal of Casting & Materials Engineering Vol. 6 No. 4 (2022) 69–75
https://doi.org/10.7494/jcme.2022.6.4.69

Optimization of Ladle Tilting Speed for Preventing Temperature Drops in the Die Casting Process

Haru Ando[a*], Daichi Minamide[a], Yuto Takagi[a], Ken'ichi Yano[a], Naoto Nakamura[b], Masahiro Sano[b], Takahiro Aoki[b], Yasunori Nemoto[c]

[a] Mie University, Faculty of Engineering, Department of Mechanical Engineering, 1577 Kurimamachiya-cho, Tsu, Mie, Japan
[b] Yamaha Motor Co Ltd, 2500 Shingai, Iwata-city, Shizuoka, Japan
[c] Flow Science Japan, Inc. Motoasakusa MN Bid.7F, 1-6-13, Motoasakusa, Taito-ku, Tokyo, Japan
**e-mail: yanolab@robot.mach.mie-u.ac.jp*

Received: 21 December 2021 /Accepted: 13 July 2022 / Published online: 22 December 2022.
This article is published with open access at AGH University Press.

Abstract

In die casting, molten metal poured into a shot sleeve is pressed into a mold by a plunger at high speed. The temperature of the metal drops significantly while it is being poured from the ladle to the shot sleeve, resulting in casting defects such as misrun flow lines. Although it is important to control the temperature at all stages of the process, a method for minimizing temperature loss has not yet been clarified to date. In this study, the cause of the temperature drop in the shot sleeve was clarified, and a method of optimizing the ladle tilting speed was proposed to prevent temperature drop. First, experiments were conducted to measure the decrease in metal temperature in the sleeve during pouring. These experiments revealed that the metal cools significantly from the moment it touches the shot sleeve. Therefore, the time from the first contact between the shot sleeve and the metal to the start of pouring was set as the objective function. A genetic algorithm was then used to derive the optimal ladle tilting speed pattern to suppress the temperature drop. This analysis confirmed that the metal was poured without flowing out or running ahead and that the immediate liquid level vibration after pouring was suppressed, thus ensuring stable pouring.

Keywords:

temperature drop, die casting, optimization, pouring, ladle tilt

1. INTRODUCTION TO THE SUBJECT AND PURPOSE OF THE RESEARCH

In die casting, when the casting temperature is too low, the flowability of the product is reduced, and casting defects such as misrun and flow line occur [1]. The problem is that the temperature of the molten metal drops significantly while it is flowing from the ladle to the shot sleeve. Therefore, a method to minimize the temperature drop at the stage before injection is necessary [2, 3].

One solution to this casting problem is to raise the temperature of the metal before injection it. However, increasing the thermal load on the shot sleeve causes cracks and shortens the life of the shot sleeve [4, 5].

A different solution is to fill the mold more quickly. To do so, the pouring speed of the ladle and the ejection speed of the plunger must be increased [6]. However, inadvertent pouring requires a waiting time for the molten metal surface in the sleeve to become static. During this time, the temperature will drop more [7].

In this research, we clarify the cause of the temperature drop when metal is poured into the shot sleeve during die casting. We then propose a pouring control input that can suppress the temperature drop during the pour and quickly proceed to the injection process. Finally, we show the effectiveness of the proposed method by comparing the derived control input with the control input used in the casting process by CFD simulation.

2. HEAT TRANSFER COEFFICIENT IDENTIFICATION FOR POURING MODEL

We conducted an experiment to measure the temperature of metal during pouring. In this research, we used a die casting machine (Shibaura Machine Co., Ltd DC135J-T). The sleeve, made of SKD61, has an inner diameter of 60 mm and a length

of 200 mm. The metal is an aluminum alloy (JIS-ADC12) with an initial temperature of 690°C and a casting weight of 0.71 kg (sleeve filling rate: 42.0%). The material properties of JIS-ADC12 are shown in Table 1. The tip of the ladle is placed 30 mm above the pouring hole of the shot sleeve and tilted to the sleeve at an angle of 45 deg.

Table 1
The material properties of JIS-ADC12

Properties	Values
Liquidus temperature	598°C
Solidus temperature	513°C
Density	2467 kg/m^3
Viscosity	0.00145 Pa·s

We installed one sheath thermocouple in the ladle and six in the shot sleeve to measure the metal temperature during pouring. The locations of the thermocouples in the sleeve are shown in Figure 1. The top parts of the sleeve, in order from shortest to longest from the pouring hole, are labeled No. 1, No. 2, and No. 3, and the bottom parts are No. 4, No. 5, and No. 6. Figure 2 shows the temperatures from the start of pouring. The start time is when the thermocouple first measures the temperature in the shot sleeve.

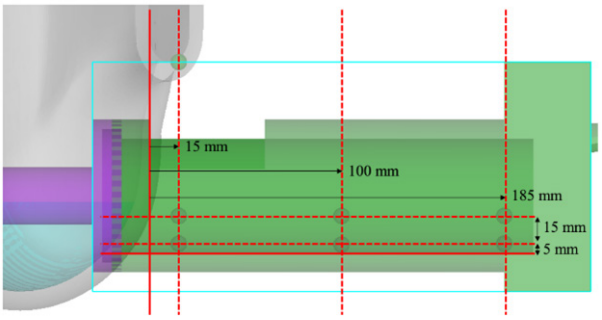

Fig. 1. Temperature measurement positions inside the shot sleeve

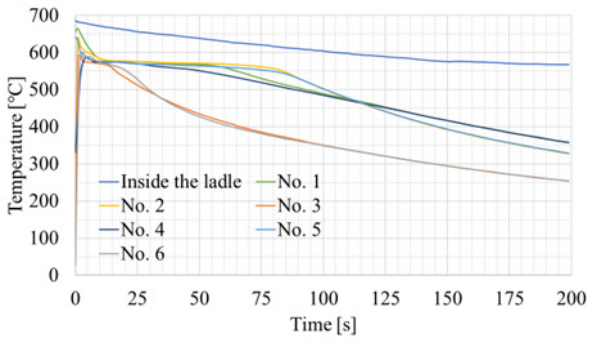

Fig. 2. Molten metal temperatures

In Figure 2, the first curve shows the time-series temperature data at the measurement points set in the ladle, and the other curves are temperature data of molten metal at the measurement points shown in Figure 1. The metal temperature in the ladle at the start of pouring is almost the same as the initial temperature. Therefore, it is assumed that the thermal diffusion from the molten metal to the air is very small during the conveyance and the tilting of the ladle.

Although the temperature at the first measurement point in the shot sleeve is close to the initial temperature, the temperature drops significantly and rapidly while the metal is being poured. After the completion of pouring, the temperature decreases slowly. This indicates that the heat transfer to the shot sleeve accounts for most of the temperature drop during pouring.

We used *FLOW-3D* from Flow Science, Inc. for CFD analysis. To construct the CFD pouring model, we needed to define the heat transfer coefficient between the metal and the shot sleeve using the experimental results. At this point, due to the time required for CFD simulation, we simulated the pouring model for 20 s from the start of tilting. In the simulation model, measurement points are set at the same six locations in the shot sleeve as in Figure 1.

Figure 2 shows that the time when the temperature peaks differs from point to point. It is assumed that this is due to the response delay of the thermocouples. Therefore, we compared the simulation results with the experimental results after the time when the peak temperature was reached, and adopted the heat transfer coefficient of the shot sleeve that shows the most similar temperature history. The value of Y is set to evaluate the similarity between the simulation results and the experimental results.

$$Y = \sum_{(i=1)}^{6} D_i \tag{1}$$

$$D_i = \sum_{(j=t_p)}^{20} (T_{ije} - T_{ija})^2 (j = t_p,\ t_p + 1, \ldots,\ 20) \tag{2}$$

Here, i is number of the six measurement points shown in Figure 1, and j is the time t_p after the peak value. For the timeline of the experiment and the simulation, t = 0 s is the time when the temperature of the metal is first measured at any of the measurement points. For each measurement point, the residual sum of squares D_i between T_{ija} [°C] (the temperature calculated from simulation) and T_{ije} [°C] (the temperature calculated from simulation) is calculated. Then, the sum of D_i values for the six measurement points is defined as the evaluation value Y. We searched for the heat transfer coefficient with the minimum value of Y by using the golden section method. For the sleeve heat transfer coefficient, the search range is 0 to 2500 W/(m^2 · K) [8, 9].

3. TEMPERATURE DECREASE FACTOR ANALYSIS

From Equations (3) and (4), equations of heat transfer quantity, Q, the heat transfer quantity [W] is derived using h, the heat transfer coefficient [W/(m^2 · K)], and its value fluctuates greatly depending on the area of fluid–solid contact A [m^2] and time t [s]. Here, T_a and T_w are the temperatures of objects in different phases.

$$Q = \int q \cdot A(t) \cdot \mathrm{d}t \tag{3}$$

$$q = h(T_a - T_w) \tag{4}$$

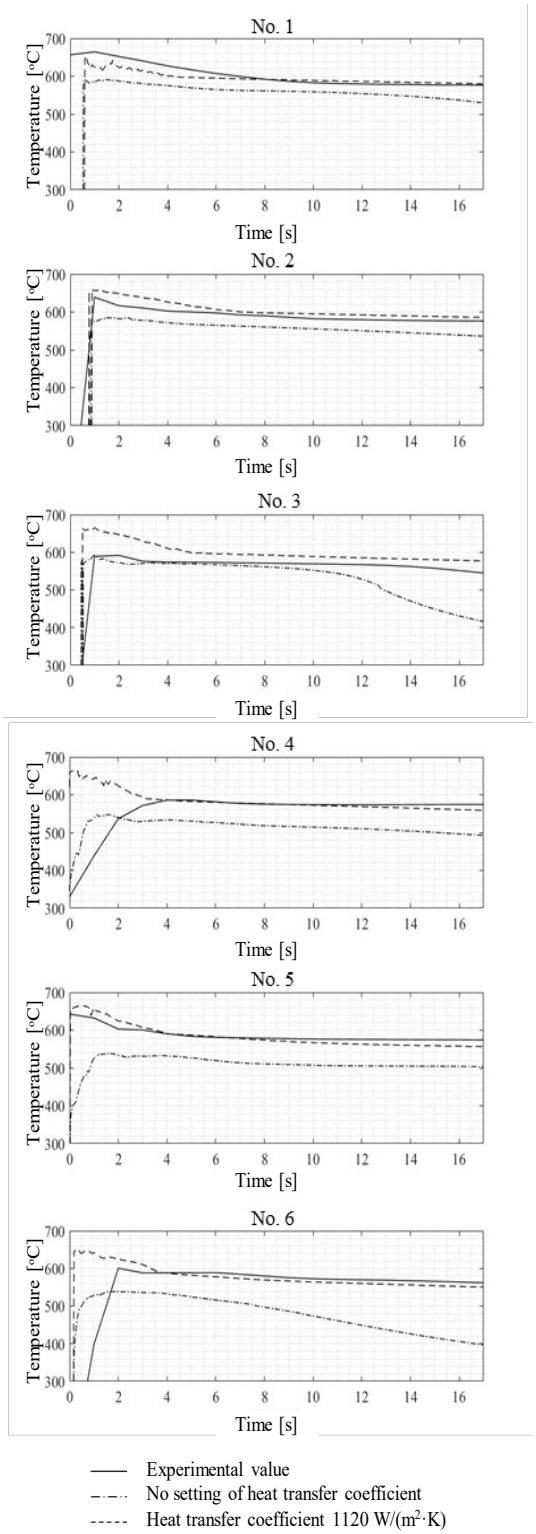

Fig. 3. Temperature comparison between experiment and CFD simulation

Figure 3 compares the simulation results and the experimental results using the obtained optimum heat transfer coefficient of 1120 W/(m^2 · K). In the case of simulation without setting the heat transfer coefficient, the thermal diffusivity is estimated from the thermal conductivity. From Figure 3, it can be confirmed that the simulation results using the derived heat transfer coefficient are sufficiently similar to the metal temperatures measured in the experiment. Therefore, the CFD simulation of the pouring model is performed using the derived heat transfer coefficient 1120[W/(m^2 · K). From the experimental results shown in Figure 3, it can be inferred that the heat transfer to the shot sleeve is much more dominant than that to the air in the temperature drop of the metal. To investigate the cause of the temperature drop, we performed CFD simulations using several tilt patterns. We then analyzed the molten metal near the inner surface of the shot sleeve, where temperature changes are large, focusing on the contact time and area with the shot sleeve. From the results, we searched for ways to improve the temperature drop. The following equation is the definition of the contact time Δt [s] between the inner surface of the sleeve and the metal. Δt is the difference between t_{first} (the time when the metal first touches the sleeve) and t_{fin} (the time when the pouring is completed).

$$\Delta t = t_{fin} - t_{first} \tag{5}$$

$$t_{\text{fin}} = \left\{ t \middle| \begin{matrix} h_{|t=t,\ldots,t_{end}|} < h_{\max} \\ t > t_{first} \end{matrix} \right\} \tag{6}$$

At the pouring completion time t_{fin} the molten metal surface must be in a static state. To determine this, t_{fin} is defined as the time when the maximum height h [m] of the molten metal surface converges to an arbitrary height $h_{\max}$ [m] or less. In this research, $h_{\max}$ is defined as the height of the metal surface at the time of static flow +10%.

The pseudo contact area of the metal with the inner surface of the shot sleeve is defined as the number of cells into which the metal flows. Figure 4 shows the relationships among the contact time and area of the metal with the inner surface of the shot sleeve and the average temperature of the metal at the time of pouring completion, obtained by CFD simulation.

As shown in Figure 4, the temperature drop depends strongly on the amount of time that the metal is in contact with the inner surface of the sleeve. This is because the contact area increases and decreases instantaneously and is not constant, so the effect on the temperature drop is small. Therefore, it is possible to suppress the drop by deriving a pouring control input that can shorten the contact time so that it quickly shifts to the injection process. In this research, we used the tilting speed input as the pouring control input and derived it by genetic algorithm (GA) optimization.

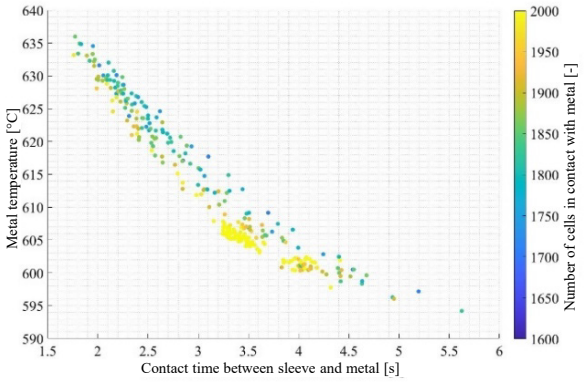

Fig. 4. Relationship between temperature drop and heat outflow to shot sleeve

4. TILTING SPEED INPUT OPTIMIZATION TO EVALUATE TEMPERATURE DROP OVER THE ENTIRE SETTABLE RANGE

The design variables of the optimization used in this research are shown in Figure 5. In the pouring system of the target die casting machine, the tilting speed is set using two speed parameters.

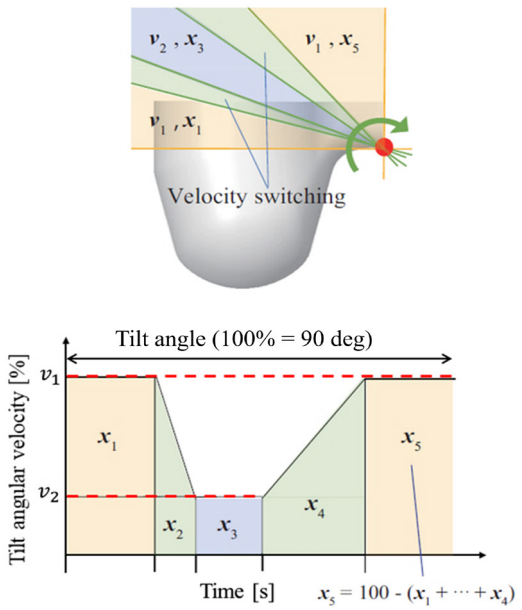

Fig. 5. Definitions of design variables for tilting speed

The parameters of the tilting speed are v_1 and v_2 [%], respectively. Due to the constraints of the die casting machine, the tilting speed input for the ladle is given in three steps, varying in the order of v_1 and v_2. These parameters are each set as a percentage of the maximum frequency of the inverter in the ladle tilt actuator, and the unit is percent. The speed parameter is temporarily denoted as [%]. If the actual tipping speed of the ladle is [rad/s], it can be converted as shown in Equation (7) from the experiment conducted by Kanazawa in this laboratory [10].

$$v' = 1.24v + 0.20 \tag{7}$$

Then, the timing of speed switching is expressed as the amount of rotation x_1, x_2, x_3, x_4 [%] in each speed interval, taking the percentage of the total rotation of the tilt. The above six variables are defined, and the simulation is carried out until 3 s after the end of the tilt.

From the above, the contact time between the inner surface of the sleeve and the molten metal was set as an alternative evaluation value to suppress the temperature drop. Then, the tilting speed input that suppresses the temperature drop is obtained by GA optimization. The evaluation functions are shown in Equations (5) and (6). t_{fin} is the time when the area of the fluid touching the inspection surface (hereinafter referred to as flow surface area) [m^2] at height h_{max} becomes less than the threshold value. As shown in Figure 6, the flow surface area increases and decreases continuously during the pouring process due to the waves returning inside the shot sleeve. Therefore, t_{fin} is determined only when the flow surface area does not exceed the threshold value at any subsequent time.

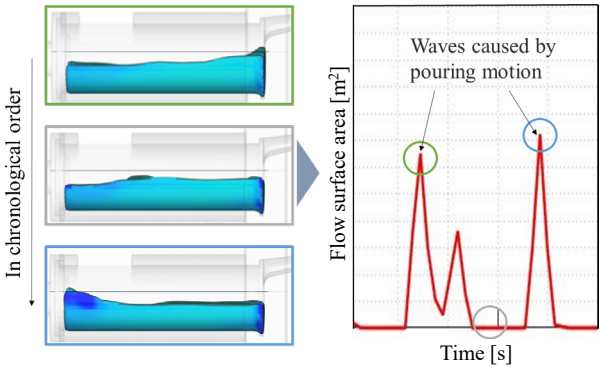

Fig. 6. Determination of pouring completion time

In this research, the threshold value is set to $3.0 \cdot 10^{-6}$ m^2 to account for calculation errors. Individuals whose liquid level oscillation does not stop by the end of the simulation are excluded from the solution.

Another constraint in the optimization was that we also excluded from the solution any individuals for which forerunning of metal or outflow outside the pouring hole of the shot sleeve was confirmed. Forerunning is a phenomenon in which the molten metal flowing into the product mold section solidifies before injection, and fragments of solidified metal flow into the inside of the product with molten metal. This phenomenon decreases product quality. In addition, if molten metal flows out of the shot sleeve pouring hole, there is a risk of deterioration in yield and a loss of safety. These two points are set as constraints on the feasibility. The location of the inspection surface is shown in Figure 7. In Figure 7a, forerunning has occurred if molten metal flows into the inspection surface installed at the sprue connected to the mold at the pouring process. In Figure 7b, an inspection surface is placed around the shot sleeve pouring hole to check for molten metal outflow.

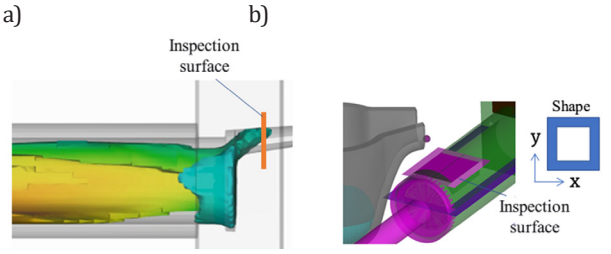

Fig. 7. The location of the inspection surface: a) forerunning inspection surface; b) outflow inspection surface outside the shot sleeve

In both conditions, the individual is evaluated only when the flow surface area of the inspection surface stays below the threshold value until the end of the simulation. The threshold value is set to $3.0 \cdot 10^{-6}$ m^2 to account for calculation errors as well as the evaluation function.

Using the evaluation function and the constraints described above, we defined the optimization problem as follows.

Minimize:

$$J(\nu, x) \tag{8}$$

Subject to:

$$0.1 \le \nu_1,\ \nu_2 \le 100 \tag{9}$$

$$0.1 \le x_1,\ x_2,\ x_3,\ x_4 \le 100 \tag{10}$$

$$I_1(t) < F_{\min 1} \tag{11}$$

$$I_2(t) < F_{\min 2} \tag{12}$$

$$F_{\min 1},\ F_{\min 2} = 3.0 \cdot 10^{-6} \tag{13}$$

The objective function J is Δt (the contact time between the inner surface of the sleeve and the molten metal), I_1 is the flow surface area of the inspection surface at the sprue, and I_2 is the flow surface area of the inspection surface around the sleeve pouring hole. The optimization problem is solved using a general GA, and the optimization parameters are shown in Table 2.

Table 2
Optimization parameters

Number of generations	6
Population	100
Elite number	20
Selection method	Tournament
Crossing method	REX

The optimization results are shown in Figures 8 and 9. A single point in these figures represents a single individual. Figure 8 shows the convergence of the solution tendency based on the number of generations and the evaluation value (the contact time between the shot sleeve and the molten metal) of each individual. Figure 9 shows the relationship between the evaluation value, the time of completion of tilting, and the average temperature at the completion of pouring.

The point in red in Figure 9 show the results of the simulation using the conventional tilting pattern.

Figure 8 shows that 14 of 100 individuals satisfied the conditions in the initial generation. This means that the range within which molten metal can be poured safely is small and that the search has been insufficient. Therefore, the parent individuals are not similar, and the results do not approach the optimal solution even if they are crossed. In addition, Figure 9 shows that child individuals tend to be generated in order to shorten the time until tilting stops, rather than the evaluation value. This is a result of the fact that the direction in which the solution population of the child individuals evolved varied due to the insufficient number of parent individuals, and therefore converged to a localized solution before reaching the optimal solution.

To improve the efficiency of the search for the optimal solution, we redefined the range of design variables. For this purpose, we analyzed the tilting patterns of the individuals with excellent optimization solutions shown in Equations (8)–(13), and determined the range of design variables in which the tilting pattern that enables stable pouring is likely to exist.

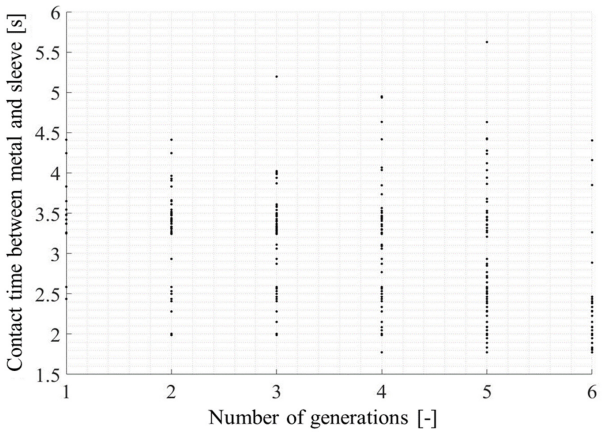

Fig. 8. Optimization convergence process

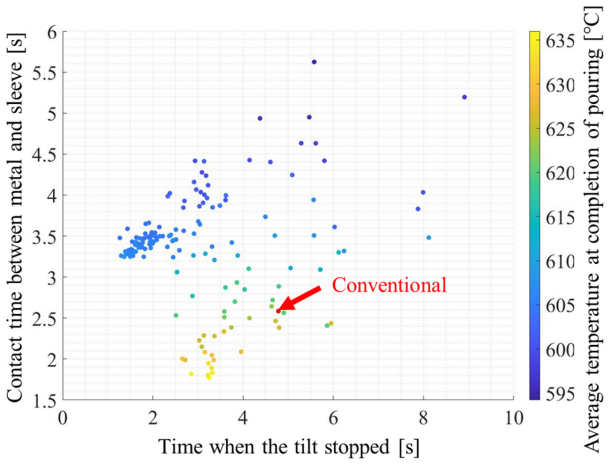

Fig. 9. Comparison of evaluation values of optimization results

5. OPTIMIZATION OF TILTING SPEED INPUT IN THE DESIGN DOMAIN CONSIDERING FEASIBILITY

Based on the optimization results described in Section 4, the relationship between the tilting speeds v_1, v_2 and the average temperature of the metal at the time of pouring completion is shown in Figure 10. Here, the x-marked solutions in the graph represent the individuals that were eliminated from the generation due to the constraint conditions, and the dots-marked group represents the individuals that were evaluated in the optimization algorithm.

From this result, it is clear that the constraint condition is rarely satisfied when both v_1 and v_2 are fast compared to other individuals. This is because the high-speed tilt causes a large disturbance in the metal behavior, thus preventing stable pouring. In the individual cases that satisfied the constraint conditions and were subject to evaluation, v_1 was relatively slow. Therefore, it is assumed that metal is poured without disturbing the liquid surface behavior because the speed slows down in the latter half of the ladle tilt when the metal starts to flow.

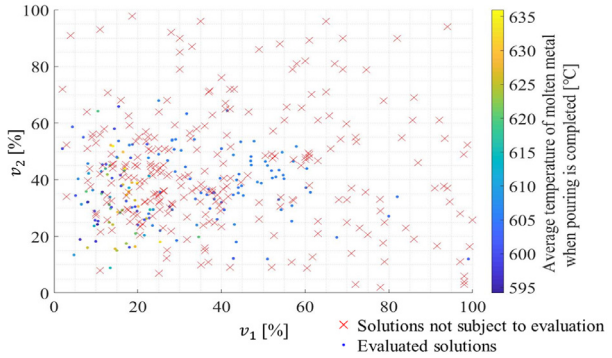

Fig. 10. Relationship between tilting speed and pouring feasibility

Based on this analysis, the range of design variables for the tilting speed was changed to the following equation in consideration of practicality.

$$0.1\% \le v_1 \le 30\% \tag{14}$$

$$0.1\% \le v_2 \le 70\% \tag{15}$$

The ladle tilting speed is optimized with the change in the range of design variables. The conditions of the optimization problem other than the tilting speed variables are in accordance with Equations (8), (10)–(13). Here, there are 50 individuals per generation, 7 generations, and 20 elite individual conservations. A general GA is used for optimization as in Section 4. The optimization results are shown in Figure 11 and Figure 12. In the figures, each point represents one individual, as in Section 3, and the red point in Figure 12 shows the result of the analysis using the conventional tilting pattern.

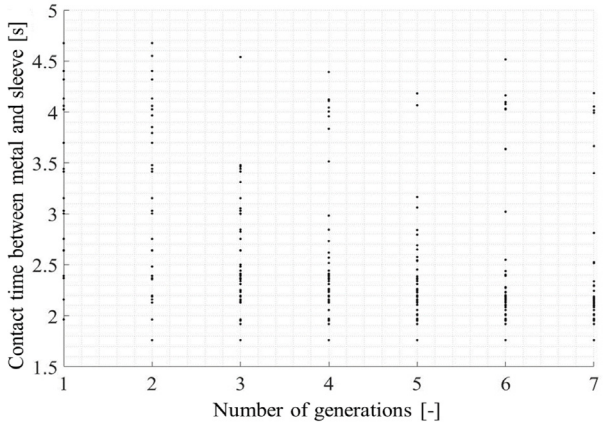

Fig. 11. Optimization convergence process

Figure 11 shows that 20 of 50 individuals satisfy the constraints in the initial generation. The percentage of feasible tilting speeds was higher than it was before the change in the range of design variables. In the second generation, 11 of 30 individuals satisfied the constraints, as did 17 of 30 in the third generation. Thus, the efficiency of the search for stable tilting speed input has been improved. From Figure 12, it can be confirmed that a solution group close to the optimum solution is formed without splitting the group. Here, we focused on the fact that the evaluation is often poor in cases where tilting stops after only a short time. This is because the shot time lag tended to become longer because the metal was violently disturbed in the shot sleeve during pouring by high-speed tilting. The same phenomenon was observed in the previous research, which guarantees the reproducibility of the CFD simulation model in this research.

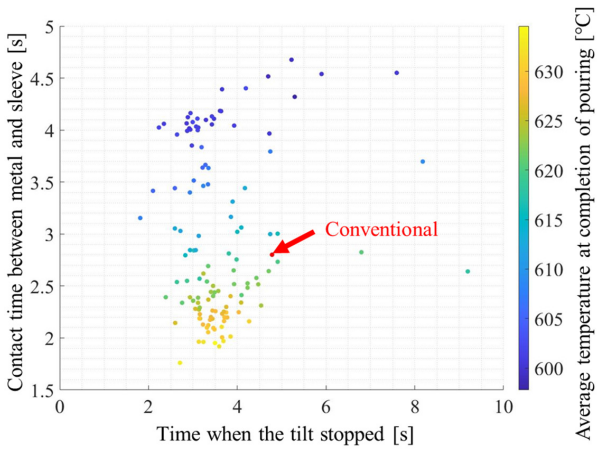

Fig. 12. Comparison of evaluation values of optimization results

The CFD simulation results of the pouring model with the optimized tilting speed input and the conventional input are shown below. Figure 13a shows the average temperature history of the metal, and Figure 13b compares the derived tilting speed input and the conventional tilting speed input used in actual die casting manufacturing.

The simulation results in Figure 13 show that the derived tilt pattern can suppress the temperature drop by 15.9°C compared to the conventional tilt pattern. The time to complete pouring was also shortened. In the design of the tilting speed input, it was clarified that the pouring could be completed while the liquid level of the metal was calm by using a high rotation speed for the first half of the ladle tilt and by extending the low-speed part in the second half.

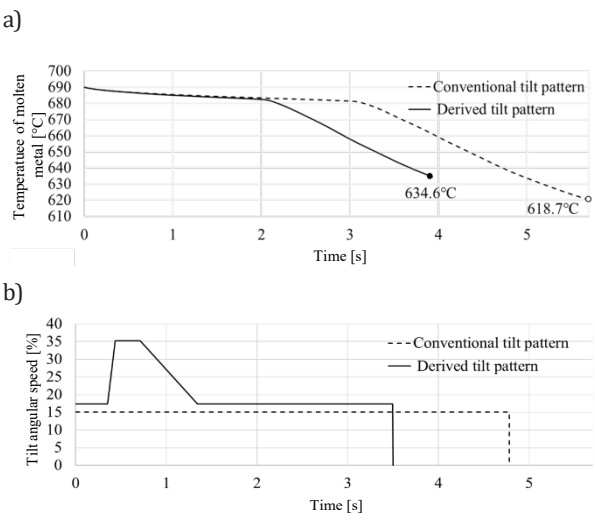

Fig. 13. The CFD simulation results of the pouring model with the optimized tilting speed input and the conventional input: a) temperature history of the metal; b) tilting speed input

6. CONCLUSIONS AND SUMMARY

In this research, we focused on the temperature drop during pouring in die casting and analyzed the factors in the drop using CFD simulation. The experiment to measure the decrease in metal temperature in the shot sleeve during pouring proved that the temperature decreases significantly from the moment the metal touches the sleeve. Therefore, the time from the first contact between the sleeve and the molten metal to the injection start time was set as the objective function, and the optimal ladle tilting speed pattern to suppress the temperature drop was derived using a genetic algorithm. The simulation confirmed that the derived tilting speed input did not cause metal to flow out or forerunning, and suppressed the turbulence of the metal surface immediately after pouring, thus ensuring stable pouring.

REFERENCES

[1] Laukli H.I., Arnberg L. & Lohne O. (2005). Effects of grain refiner additions on the grain structures in HPDC A356 castings. *International Journal of Cast Metals Research*, 18(2), 65–72. Doi: https://doi.org/10.1179/136404605225022919.

[2] Yu W., Cao Y., Guo Z. & Xiong S. (2016). Development and application of inverse heat transfer model between liquid metal and shot sleeve in high pressure die casting process under non-shooting condition. *China Foundry*, 13, 269–275. Doi: https://doi.org/10.1007/s41230-016-5137-4.

[3] Sugihara T., Fujishiro M. & Maeda Y. (2019). Direct Observation and simulation of ladle pouring behaviour in die casting sleeve. *VI International Conference on Particle-Based Methods: fundamentals and applications, 28–30 October, Barcelona*. Barcelona: CINME, 610–618.

[4] Vachhani H., Rathod M. & Shah R. (2019). Dissolution and erosion behavior of AISI H13 shot sleeve in high pressure die casting process. *Engineering Failure Analysis*, 101, 206–214. Doi: https://doi.org/10.1016/j.engfailanal.2019.02.021.

[5] Abid D., Ktari A., Mellouli D., Gafsi N. & Haddar N. (2019). Failure analysis of shot–sleeves used in brass high pressure die–casting process. *Engineering Failure Analysis*, 104, 177–188. Doi: https://doi.org/10.1016/j.engfailanal.2019.05.038.

[6] Korti A.I.N. & Abboudi S. (2017). Effects of shot sleeve filling on evolution of the free surface and solidification in the high-pressure die casting machine. *International Journal of Metalcasting*, 11(2), 223–239. Doi: https://doi.org/10.1007/s40962-016-0051-5.

[7] Iwata Y., Dong S., Sugiyama Y. & Iwahori H. (2013). Effects of solidification behavior during filling on surface defects of aluminum alloy die casting. *Materials Transactions*, 54(10), 1944–1950. Doi: https://doi.org/10.2320/matertrans.F-M2013819.

[8] Helenius R., Lohne O., Arnberg L. & Laukli H.I. (2005). The heat transfer during filling of a high-pressure die-casting shot sleeve. *Materials Science and Engineering: A*, 413–414, 52–55. Doi: https://doi.org/10.1016/j.msea.2005.08.166.

[9] Yu W., Cao Y., Li X., Guo Z. & Xiong S. (2017). Determination of interfacial heat transfer behavior at the metal/shot sleeve of high pressure die casting process of AZ91D Alloy. *Journal of Materials Science & Technology*, 33(1), 52–58. Doi: https://doi.org/10.1016/j.jmst.2016.02.003.

[10] Kanazawa K. (2015). *Nonparametric shape optimization methods using parametric curves*. Graduate School. Mie University [Doctoral Dissertation].